Frontiers in Health InformaticsISSN-Online: 2676-7104
www.healthinformaticsjournal.com
2024; Vol 13: Issue 7
Open Access

Bayesian-Optimized Caries Classification in Dental Radiographs Using Mask R-CNN

[1]Dr. Aakanksha Mahajan, [2]Dr. Suman, [3]Dr. Rajiv Arora and [4]Piyush Batra
[1]Associate Professor, PIET, Samalkha
[2]Associate Professor, BPIT, Delhi
[3]Associate Professor, ADGIPS, Delhi
[4]Assistant Professor,ADGIPS, Delhi

Cite this paper as:
Aakanksha Mahajan, Suman, Rajiv Arora and Piyush Batra (2024). Bayesian-Optimized Caries Classification in Dental Radiographs Using Mask R-CNN. *Frontiers in Health Informatics,* 13(7), 527-552

ABSTRACT
In order to improve diagnostic speed and accuracy, dental image analysis has become a crucial topic of study in the field of dentistry, utilizing developments in computer vision and machine learning. Manual evaluation is frequently used in traditional dental diagnosis techniques, which can be laborious and prone to human mistake. Because dental diseases, especially caries (tooth decay), are becoming more complicated, automated solutions that offer trustworthy and impartial assessments are required. This study presents a special technique that effectively analyzes many dental images while placing great emphasis on the identification and classification of multiple types of caries. Using sophisticated deep learning techniques, the Mask Region-based Convolutional Neural Network (Mask R-CNN) is employed effectively, allowing for efficient isolation and accurate segmentation of individual teeth in multiple dental images. A variety of three different techniques after performing segmentation is also applied, to effectively extract many relevant features, including Histogram of Oriented Gradients (HOG), Gabor Filters, along with Extreme Features (X-Feat). Each feature extraction method catches special aspects of tooth shape, so the classification approach becomes more strong. The retrieved features are categorized with a Bayesian-Optimized Random Forest Classifier. This helps to increase the precision of identifying dental conditions. This all-all-embracing technique provides accurate and automatic evaluations for multiple dental issues and it simplifies customary dental diagnostics. The findings show that this method classifies dental diseases. It can classify caries and other dental diseases with a maximum accuracy of 98.08%.

Keywords – *Bayesian-Optimization, Gabor Filters, HOG, Mask R-CNN, Random Forest, X-Feat.*

I. INTRODUCTION

Dental image segmentation is crucial in modern dental care, particularly for diagnosis, treatment planning, and monitoring the patient condition. With the advent of digital imaging technology and artificial intelligence, there is a rapid progress in the field of dental image analysis, offering more accuracy and efficacy in the segmentation of teeth from dental radiographs and other imaging modalities [1]. Despite these advancements in the field, dental picture segmentation remains challenging due to the intricacies of dental anatomy, the complexity of the oral cavity, and varying image quality. The development of accurate and automated segmentation techniques is essential since the current manual segmentation methods are time-consuming, labor-intensive, and prone to human error [2].

Early methods of segmenting dental images mostly depended on traditional image processing methods, which were unable to handle the wide range of tooth sizes, shapes, and occlusions. For a number of uses in dental image analysis, including cavity detection, orthodontic treatment planning, tooth identification, dental charting, and oral disease monitoring, tooth segmentation is essential [3] [4]. Early approaches such as region-based algorithms, edge detection, and thresholding were frequently constrained by poor contrast, noise, and the

significant differences between individual teeth. With the potential to extract intricate patterns from massive datasets, machine learning and deep learning techniques have become more popular over time, resulting in more automatic and precise segmentation [5].

The Mask R-CNN architecture, which builds on Faster R-CNN by adding a branch for segmentation masks in addition to bounding boxes, has been one of the most promising developments in this field [6] [7]. In object instance segmentation, including applications in medical imaging, Mask R-CNN has demonstrated noteworthy results [8]. It is especially well-suited for dental image analysis, where precisely defining individual teeth is crucial, due to its capacity for pixel-level segmentation. When it comes to intricate dental structures, occlusions, and different tooth morphologies, this approach works quite well. To distinguish areas of interest, such individual teeth, from the backdrop and other irrelevant regions in dental images, the segmentation stage is crucial.

However, segmentation by itself is insufficient for a thorough study. The next crucial stage is feature extraction, which makes it possible to retrieve useful information from the segmented images. This makes it possible to do tasks like anomaly detection and categorization with greater accuracy. In order to differentiate between different dental problems, effective feature extraction techniques record important features such the size, shape, texture, and orientation of teeth. To increase classification accuracy, feature extraction must be made more robust.

By employing Mask R-CNN for segmentation and sophisticated feature extraction techniques to enhance the precision and dependability of dental image analysis, this study expands on existing developments. With its strong pixel-level instance segmentation capabilities, Mask R-CNN is especially well-suited for dental images where accurate tooth separation is essential. Complex structures, overlapping teeth, and a variety of tooth forms may all be handled by its design. More in-depth examination of the segmented regions is provided by feature extraction, which is based on the segmentation.

We use three complementing methods—the Histogram of Oriented Gradients (HOG), the Gabor Filter, and Extreme Features (X-Feat)—to extract significant features. In order to identify certain dental features, X-Feat is made to capture the teeth's distinctive geometric structures, such as cusps, ridges, and curves. A texture-based descriptor, the Gabor Filter extracts orientation and frequency information from dental images. Because of the intricate surface structures and variances in tooth morphology, it is especially helpful in accurately identifying the textures and patterns seen in teeth. By producing a collection of answers at various sizes and orientations, gabor filters enable us to obtain a thorough depiction of the tooth textures.Gradient orientation is the main focus of HOG, which captures minute structural features like the curvature and texture patterns that distinguish different dental states and characterize individual teeth.

Following feature extraction, a Bayesian-Optimized Random Forest is used to classify the merged feature set. For precise classification, the Random Forest method, which is renowned for its resilience, builds many decision trees and combines their predictions. This is further improved by Bayesian optimization, which optimizes the classification performance by adjusting hyperparameters like the number of trees and their depth. Our method's accuracy and efficiency are guaranteed by the combination of sophisticated feature extraction and classification, which also makes it flexible enough to accommodate different dental conditions and image features.

A thorough approach to dental image segmentation and analysis is offered by combining Mask R-CNN for segmentation with sophisticated feature extraction techniques including X-Feat, Gabor Filter, and HOG, followed by classification using Bayesian-Optimized Random Forest. Key issues including human annotation, segmentation accuracy, and variability in dental images are addressed by this technique. This method has the potential to greatly enhance dental diagnostics by providing an automated, precise, and reliable system, making it a useful tool for dental practitioners in actual clinical situations.

Developing a comprehensive and technically sophisticated system for dental image segmentation and classification using cutting-edge segmentation and feature extraction approaches is the main contribution of this

study.

- ***Segmentation using the Mask Region-based Convolutional Neural Network (Mask R-CNN):*** Mask R-CNN is used to segment teeth at the pixel level, handling intricate dental occlusions and structures with ease. The segmentation procedure is more accurate and dependable because to this method's exact delineation of individual teeth.
- ***Hybrid Feature Extraction*** A rich, multi-dimensional feature set is produced by combining the complementing feature extraction methods of X-Feat, Gabor Filter, and HOG. HOG records gradient orientation, Gabor Filter concentrates on texture representation across different orientations and scales, and X-Feat records geometric features. When combined, these techniques guarantee that strong and discriminative features are extracted from dental images.
- ***For optimal classification, a Bayesian-Optimized Random Forest*** is used to classify the combined feature set following feature extraction. By adjusting the hyperparameters to maximize performance, this guarantees that the classification is accurate and effective.

Through the combination of sophisticated segmentation and feature extraction methods with optimal classification, this study presents a revolutionary approach to dental image analysis. These contributions advance the field of dental image segmentation and give dentists access to a more accurate and effective diagnostic tool.

Section 2 of the paper starts with a thorough literature review that covers pertinent studies in the field of dental image segmentation and categorization. The approach is described in full in Section 3, which also explains the suggested strategies and how they were put into practice. The experiments' results are shown in Section 4, which is followed by a thorough examination of their importance. Section 5 wraps up the investigation by summarizing the main conclusions and offering closing thoughts.

II. LITERATURE REVIEW

Innovative techniques that greatly improve diagnostic precision and treatment planning have been incorporated into dental image segmentation in recent years. In this field, the application of deep learning techniques has become a game-changing strategy. The U-Net architecture is a noteworthy technique that has been effectively used for radiographic image segmentation of dental structures. For instance, U-Net outperforms conventional methods in handling the segmentation of occluded teeth, as shown by the authors of [9], who achieved a better accuracy rate under a variety of imaging situations.

Likewise, segmentation performance has been enhanced by the use of Generative Adversarial Networks (GANs). The possibility of GANs to produce artificial dental images was investigated by the authors of [10], who aimed to improve segmentation outcomes by expanding the training dataset. By addressing the issue of sparsely annotated data, their method improved the model's generalization across several dental imaging modalities [10].

Recent research has also placed a lot of emphasis on the integration of multimodal imaging methods. For better tooth segmentation, the authors of [11] suggested a hybrid approach that combines panoramic radiography and cone beam computed tomography (CBCT). Their approach used the advantages of both imaging modalities by using a two-stream convolutional neural network (CNN) architecture, which resulted in improved segmentation accuracy [11].

Adding attention techniques to segmentation frameworks has become popular as a way to improve performance. An attention U-Net model was presented by the authors of [12] for accurate dental image segmentation. The model's accuracy was enhanced, especially in noisy images, by the attention mechanism, which allowed it to focus on important elements while lessening the impact of irrelevant information [12].

In the field, transfer learning has also shown to be a useful tactic. To improve dental image segmentation, the authors of [13] used transfer learning using CNN models that had already been trained, including ResNet and

VGG. Their results showed notable gains in segmentation accuracy, proving that using well-established models for specific dental tasks is useful [13].

There has also been potential in combining deep learning models with conventional image processing methods. In order to improve the delineation of teeth in difficult dental images, the authors of [14] combined CNN-based segmentation with adaptive thresholding and morphological procedures. Their hybrid method produced more accurate segmentation by successfully lowering noise and improving the quality of the input images [14].

Recently, self-supervised learning methods have become a promising approach to segmentation problems. To improve feature representation for dental image segmentation, the authors of [15] created a self-supervised system that makes use of contrastive learning. By using unannotated data, the model was able to learn and sustain competitive performance while relying less on labeled samples [15].

Another area of interest has been the use of hybrid feature extraction techniques. The authors of [16] achieved significant gains in segmentation accuracy and resilience by combining Local Binary Patterns (LBP) and Histogram of Oriented Gradients (HOG) for texture extraction [16].

For dental image analysis, the authors of another study used a hybrid feature extraction method that included the Fourier Transform and Wavelet Transform, showing improved segmentation performance in a variety of imaging settings [17].

Furthermore, it has been demonstrated that using ensemble learning techniques can make segmentation models more resilient. Through collaborative learning, the authors of [18] created an ensemble model that included several deep learning architectures, improving segmentation accuracy [18].

Additionally, the application of Reinforcement Learning (RL) to segmentation task optimization has been studied recently. By using RL approaches to dynamically modify model parameters during training, the authors of [19] greatly improved the segmentation of intricate dental images [19].

Dental image segmentation has advanced as a result of the introduction of 3D imaging technology. In order to segment teeth in CBCT images, the authors of a research used 3D convolutional neural networks, which demonstrated encouraging results in precisely detecting dental components in three-dimensional space [20].

Furthermore, using a hybrid model that integrated CNNs and recurrent neural networks (RNNs) to capture both spatial and temporal features, the authors of [21] examined the potential of deep learning for segmenting periodontal disease from dental images.

Another important area of research has been the integration of noise reduction methods. By improving the quality of input data, the authors of [22] suggested a unique denoising autoencoder as a preprocessing step for dental images, which increased segmentation accuracy [22].

There has also been an increase in interest in research on the segmentation of impacted teeth. A machine learning-based method for automatically identifying impacted teeth in panoramic radiographs was presented by the authors of a research in which they achieved excellent sensitivity and specificity [23].

Furthermore, research into explainable AI (XAI) methods has shown promise as a means of boosting confidence in dental image interpretation. In order to promote openness and comprehension, the authors of [24] used XAI techniques to shed light on how deep learning models make decisions when performing dental segmentation tasks.

It has been investigated to integrate cloud-based systems for group analysis of dental images. The potential of using technology in clinical settings was demonstrated by the authors of [25], who created a cloud-based solution that enables real-time cooperation among dental experts for better diagnosis and treatment planning [25].

Dental image segmentation is a fast developing subject with a wide range of approaches, including deep learning, hybrid models, conventional image processing, and sophisticated feature extraction techniques. These

developments open the door to better patient care and treatment planning in addition to increasing the precision of dental diagnostics.

The effectiveness of deep learning methods in identifying dental caries was demonstrated by the authors of [26], who used the U-Net architecture for infection identification in a dental dataset. Their solution outperformed conventional techniques with a noteworthy accuracy rate of 94.3%, highlighting the potential of deep learning to improve diagnostic accuracy in dental clinics [26]. The U-Net model's vulnerability to overfitting, particularly when trained on short datasets, is a drawback, though, and might result in less accurate predictions in clinical situations.

Using cone beam computed tomography (CBCT) images, the authors of [27] concentrated on the diagnostic potential of deep learning algorithms for morphological categorization of the distal roots of the mandibular first molar. According to their analysis, the deep learning system achieved an accuracy of 86.9%, and 21.4% of distal roots had an extra root [27]. Notwithstanding these encouraging outcomes, the study made clear that deep learning methods can have trouble identifying abnormalities that differ much from the training set, which might result in missed diagnoses in complicated situations.

To aid in automated tooth recognition, the authors of [28] made a noteworthy contribution by compiling a collection of 1500 panoramic dental images. After testing a number of segmentation algorithms, they discovered that the iterative CNN approach performed best, with an accuracy rate of 92.08% [28]. This demonstrates the increasing significance of standardized datasets in promoting dental diagnostics research and real-world applications. The findings' generalizability is constrained by the dataset's homogeneity, which could not accurately reflect the variation seen in actual clinical images.

Research Gap: Dental image segmentation techniques have advanced significantly, however there are still a number of issues that need to be resolved. The usefulness of many current approaches in clinical situations, where data may be limited or inconsistent, is limited by their heavy reliance on certain imaging modalities or their requirement for large labeled datasets. Furthermore, complex dental features are sometimes difficult for typical segmentation approaches to precisely define, especially when there is noise or tissue overlap. Strong feature extraction techniques that can capture the fine features of dental images while guaranteeing high classification accuracy are still required, notwithstanding the promise demonstrated by deep learning models.

By using Bayesian-Optimized Random Forest for improved classification, hybrid feature extraction methods, and Mask R-CNN for accurate segmentation, our suggested method seeks to close these gaps. In addition to addressing the shortcomings of current techniques, this all-inclusive framework enhances the precision and effectiveness of dental image analysis in practical applications.

III. PROPOSED METHODOLOGY

The three main steps of the technique described for dental image analysis and segmentation in this study are segmentation, feature extraction, and classification. It is a methodical and structured approach. Together, these phases guarantee the precise identification and categorization of dental caries and other associated disorders. Mask R-CNN-based segmentation, which effectively separates individual teeth from dental images, such as radiography or other imaging modalities, is the first step in the procedure. Only the pertinent areas—that is, individual teeth—are processed further for analysis thanks to this pixel-level segmentation.

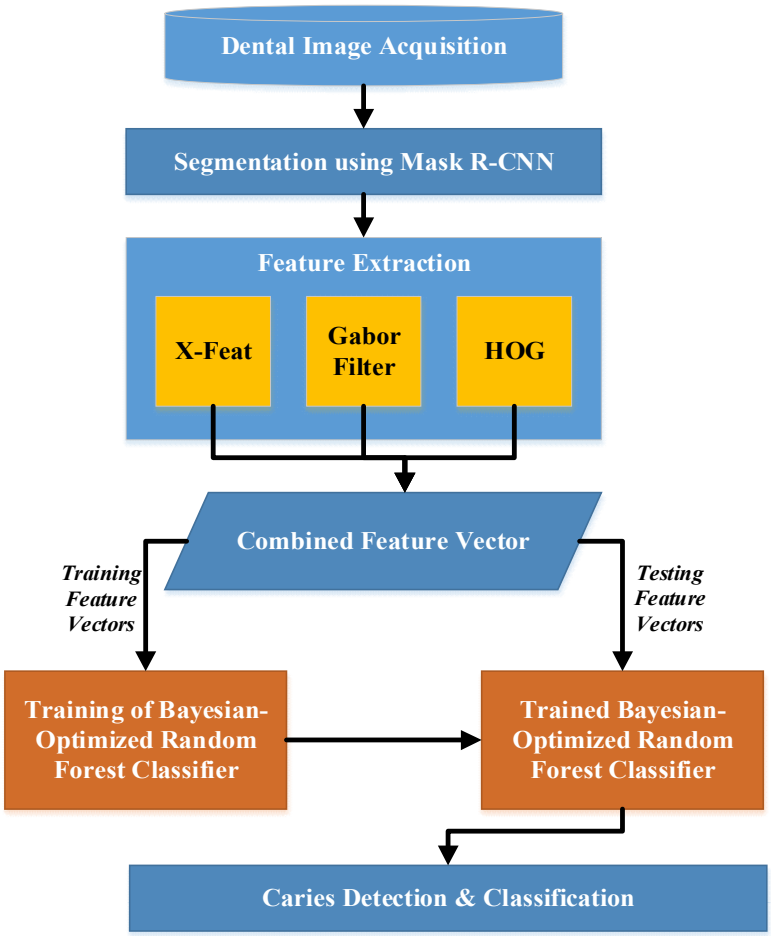

Figure 1: Workflow for proposed Dental Caries Detection and Classification

After segmentation is finished, feature extraction becomes the main emphasis. Here, we use Extreme Features, Gabor Filter-based extraction, and HOG as three complementing approaches to guarantee a thorough representation of the oral structures. Every method captures different facets of the dental image:

- Important geometric features like cusps, ridges, and curves are captured by X-Feat and are essential for distinguishing between various teeth and identifying abnormalities.
- Gabor Filters capture features that help identify dental problems including caries and structural damages by focusing on texture and spatial frequency.
- In order to identify the general form and structure of teeth, HOG highlights edges and contours by capturing gradient orientations.

Together, these extracted features provide a comprehensive feature vector that captures the different structural, textural, and geometric components of the segmented teeth.

Classification is the process's last phase. A Bayesian-Optimized Random Forest classifier uses its ensemble of decision trees to carry out the classification job after receiving the extracted feature vectors as input. High accuracy in identifying dental caries and other diseases is ensured by optimizing this classifier's prediction performance through the use of Bayesian hyperparameter tuning. The model can recognize numerous kinds of abnormalities and categorize teeth into pertinent groups, such healthy or caries-affected, thanks to the classifier's capacity to generalize across a range of dental diseases.

The entire workflow is shown graphically in Figure 1, which begins with the Image Acquisition stage and moves on to Segmentation, Feature Extraction, and Classification. This block diagram ensures a thorough and correct analysis procedure from beginning to end by showing how each stage contributes to the reliable detection and categorization of dental caries and other dental irregularities.

3.1 *Image Acquisition from Dataset*

The first step in this study is to acquire images from a carefully selected collection of dental radiographs. The majority of the images in the collection are panoramic, bitewing, and periapical images, which are often utilized in dental diagnostics. These images offer thorough perspectives of dental anatomy, and each modality has a unique diagnostic function. All of the teeth and associated bone structures are visible in panoramic images, which provide a comprehensive image of both jaws. While bitewing images emphasize the crowns of both upper and lower teeth, periapical views concentrate on individual teeth, revealing features such as root anatomy.

To guarantee that the segmentation and classification models perform well in general, the dataset comprises a range of dental diseases. These ailments include periodontal illnesses, dental implants, orthodontic procedures, tooth rot, and missing teeth. A corresponding ground truth segmentation mask is supplied for every dental image. These masks direct the segmentation process by designating each pixel as either background or tooth.

Let the dataset $D = \{(I_1, G_1), (I_2, G_2), \dots, (I_N, G_N)\}$, where:

- I_i represents the i^{th} dental image in the dataset, with $i = 1,2, \dots, N$.
- G_i is the corresponding ground truth segmentation mask for I_i, where each pixel in the mask $G_i(x, y)$ is labeled as 1 (tooth) or 0 (background).

Each image I_i has dimensions $W \times H$, where W and H represent the width and height of the image, respectively.

The dataset captures real-world variations in lighting, noise, and resolution, ensuring the model is robust against these variations during segmentation and classification.

3.2 *Image Segmentation using Mask R-CNN*

In this research, Mask R-CNN is employed for image segmentation. This advanced deep learning model extends the Faster R-CNN framework by adding a mask branch for pixel-level segmentation, making it particularly effective in segmenting teeth from dental radiographs [8].

3.2.1 Mask R-CNN Architecture

Mask R-CNN consists of several key components:

- ***Backbone Network:*** A deep convolutional neural network (e.g., ResNet-50 or ResNet-101) is used to extract feature maps from the input dental image.
- ***Region Proposal Network (RPN):*** The RPN generates a set of regions of interest (ROIs), which are likely to contain teeth.
- ***ROI Align and Classification:*** For each region, a fixed-size feature map is extracted and passed to the classification head to predict whether the region contains a tooth and to refine the bounding box (the rectangle enclosing the tooth).
- ***Mask Head:*** This branch predicts a binary segmentation mask for each region, providing pixel-level accuracy in identifying the tooth's boundaries.

3.2.2 Mathematical Formulation

Mask R-CNN involves multiple stages, each with a specific mathematical formulation.

- ***Feature Extraction using Backbone Network:*** For an input image I of size $W \times H \times 3$ (where W is the width, H is the height, and 3 represents the color channels), the backbone network extracts a feature map $F \in \mathbb{R}^{W_f \times H_f \times C_f}$, where W_f and H_f are the dimensions of the feature map, and C_f is the number of feature channels.
- ***Region Proposal Network (RPN):***The RPN proposes regions of interest by generating anchor boxes. Each anchor box is described by a 4-tuple $b_i = (x_i, y_i, w_i, h_i)$, where x_i and y_i represent the coordinates of the top-left corner, and w_i and h_i represent the width and height.

For each anchor box, two outputs are produced:

- **Objectness Score $P(b_i)$:** The probability that the region contains a tooth.
- ***Bounding Box Refinement:*** A regression function that refines the coordinates of the bounding box.

The loss function for RPN is a combination of classification loss (for object detection) and bounding box regression loss [8]:

$$L_{RPN} = \frac{1}{N_{cls}} \sum_i L_{cls}(P_i, P_i^*) + \frac{1}{N_{reg}} \sum_i P_i^* L_{reg}(t_i, t_i^*)$$

(1)

Where:

- P_i is the predicted objectness score for the i^{th} anchor.
- P_i^* is the ground truth label (1 for tooth, 0 for background).
- t_i represents the predicted bounding box, and t_i^* represents the ground truth.
- N_{cls} and N_{reg} are normalization terms for classification and regression, respectively.

- ***ROI Align and Classification:*** For each region of interest (ROI)b_i, a fixed-size feature map is extracted using ROI Align. The region is classified as either tooth or background using a softmax function, and the bounding box coordinates are refined further.

The classification loss L_{cls} and the bounding box regression loss L_{bbox} are computed as [8]:

$$L_{cls} = -\log P_{cls}^*$$

(2)

$$L_{bbox} = \text{smooth}_{L_1}(t_i - t_i^*)$$

(3)

Where P_{cls}^* is the ground truth class (tooth or background), and smooth_{L_1} is the smooth L1 loss for bounding box refinement.

- ***Mask Prediction:*** The mask branch outputs a binary mask for each detected tooth. The mask loss L_{mask} is computed using pixel-wise binary cross-entropy [8]:

$$L_{mask} = -\frac{1}{m^2} \sum_{x=1}^{m} \sum_{y=1}^{m} \left[G(x,y) \log M(x,y) + \left(1 - G(x,y)\right) \log\left(1 - M(x,y)\right) \right]$$

(4)

Where:

- $M(x, y)$ is the predicted mask value for pixel (x, y).
- $G(x, y)$ is the ground truth value (1 for tooth, 0 for background).

3.2.3 Total Loss Function

The overall loss function of Mask R-CNN combines the losses from the RPN, bounding box refinement, classification, and mask prediction:

$$L_{total} = L_{RPN} + L_{cls} + L_{bbox} + L_{mask}$$

(5)

This total loss ensures that the model effectively learns to propose regions, classify objects, refine bounding boxes, and generate accurate pixel-level masks for teeth.

3.3 *Feature Extraction*

The next stage of our study is to extract discriminative and significant features from the segmented areas of the dental images after they have been segmented using Mask R-CNN. In dental analysis, the retrieved features form the basis for precise categorization and anomaly detection. Three feature extraction methods were used in this study: Histogram of Oriented Gradients (HOG), Gabor Filter, and Extreme Features (X-Feat). A rich and complete depiction of the teeth is produced by combining the complimentary features of the dental anatomy captured by each approach. These methods are especially made to deal with the intricacies of dental images, such as the different tooth morphologies, textures, and forms.

3.3.1 Extreme Features (X-Feat) Extraction

In order to capture the cusps, ridges, and curves of teeth—all of which are essential for distinguishing between various types of teeth and identifying dental anomalies—we developed the Extreme Features (X-Feat) approach [29] in this work. These extreme features, which serve as crucial markers in the morphology of each tooth, correlate to the critical locations where the curvature of the dental structures varies substantially.

- ***Key Point Detection:***We used the Harris corner detection technique, which is very good at locating regions with large variations in image intensity, such corners or intersections, to find important locations that reflect extreme features. The Harris response function $R(x, y)$ is calculated for every pixel in the image in the manner described below [29]:

$$R(x, y) = \det(M) - k \cdot \left(trace(M)\right)^2$$

(6)

Where:

- A 2×2 matrix called the structure tensor, or M, encodes the image's gradients in both the x and y directions.
- k is the sensitivity constant (typically set to 0.04 to 0.06).

The structure tensor M is defined as [29]:

$$M = \begin{bmatrix} I_x^2 & I_x I_y \\ I_x I_y & I_y^2 \end{bmatrix}$$

(7)

Where I_x and I_y are the gradients of the image in the x and y-directions, respectively. The Harris response function highlights points where the local image structure exhibits significant variations in intensity, making it suitable for identifying prominent geometric features in teeth.

- ***Key Point Selection:*** The Harris response function $R(x, y)$ value is used to determine the selection of the main points. Extreme features are defined as points where $R(x, y)$ beyond a certain threshold. These points correlate to regions that are crucial for characterizing the morphology of the tooth, such as corners, ridges, and cusps, which are the pointy portions of teeth.
- ***Feature Vector Construction:*** The X-Feat feature vector is built using the coordinates and intensities of the chosen key points. Let $\{(x_i, y_i)\}$ stand for the collection of important points found in the image. [29] provides the final X-Feat feature vector, X_{feat}:

$$X_{feat} = \{(x_1, y_1, R(x_1, y_1)), (x_2, y_2, R(x_2, y_2)), \dots, (x_n, y_n, R(x_n, y_n))\}$$

(8)

Where n is the total number of key points. The geometric position and importance of the tooth's extreme points are encoded in this feature vector.

The technology can distinguish between various tooth kinds and diseases, such cavities or fractures, which frequently show up as geometric abnormalities, according to the X-Feat method's effective capture of the teeth's essential structural features.

3.3.2 Gabor Filter-based Features Extraction

In this work, we extracted texture-based features from dental images using Gabor filters [30]. Because of their exceptional ability to analyze spatial frequency and orientation information, gabor filters are especially well-suited for the analysis of dental images, where texture is essential for differentiating between various dental diseases.

Mathematical Formulation

The Gabor filter is mathematically defined as a sinusoidal wave (a plane wave) modulated by a Gaussian envelope. The two-dimensional Gabor function is expressed as follows [30]:

$$g(x, y; \theta, \lambda, \sigma, \gamma) = \frac{1}{2\pi\sigma^2} e^{-\frac{x'^2+\gamma y'^2}{2\sigma^2}} e^{j\left(2\pi\frac{x'}{\lambda}\right)}$$

(9)

Where:

- $x' = x\cos(\theta) + y\sin(\theta)$
- $y' = -x\ \sin(\theta) + y\ \cos(\theta)$
- θ: Orientation of the filter (0°, 45°, 90°, 135° degrees)
- λ: Wavelength of the sinusoidal factor, which controls the frequency of the Gabor filter.
- σ: Standard deviation of the Gaussian envelope, controlling the spatial extent of the filter.
- γ: Spatial aspect ratio, defining the ellipticity of the filter.

Feature Extraction Process

- ***Creation of Gabor Filter Bank:*** Several Gabor filters with different orientations (θ) and frequencies (λ) are combined to form a filter bank. The different texture patterns found in the dental images may be captured thanks to this multi-scale technique. We chose three different wavelengths and four different orientations for our investigation, yielding a total of twelve possible Gabor filters.
- ***Convolution Operation:***The input dental image is convolved with each of the gabor filters in the filter bank. The following is a definition of the convolution operation [30]:

$$\text{Response}(x,y) = (I * g)(x,y) = \sum_{u=-\infty}^{\infty} \sum_{v=-\infty}^{\infty} I(u,v) g(x-u, y-v)$$

(10)

This procedure creates a response map for every filter, highlighting distinct texture elements according to the scale and orientation of the filter.

- ***Statistical Measures for Feature Vector Construction:***Following the acquisition of the response maps, we computed a number of statistical metrics in order to create a feature vector from the filtered images. Among the salient features extracted were [30]:

- ***Mean Response:***

$$Mean = \frac{1}{N} \sum_{i=1}^{N} R_i$$

(11)

Here,R_i symbolizes the response of the i^{th} filter.

- ***Variance:***

$$Variance = \frac{1}{N} \sum_{i=1}^{N} (R_i - Mean)^2$$

(12)

- ***Energy:***

$$Energy = \sum_{i=1}^{N} R_i^2$$

(13)

- ***Entropy:***

$$Entropy = -\sum_{i=1}^{N} P_i \log(P_i)$$

(14)

Here,$P_i$symbolizes the normalized response.

- ***Combining Features:*** A thorough feature vector that captures the textural properties of the dental images was created by concatenating the features that were derived from each of the Gabor filters. Subsequent classification tasks are based on this composite feature vector.

We used the Gabor filter extraction features to improve our capacity to accurately categorize dental problems. These features provide crucial information for identifying cavities, differentiating between good and diseased teeth, and scheduling orthodontic procedures.

We greatly enhanced the texture analysis of dental images by incorporating Gabor filter-based features into our methods. Our dental image segmentation and analysis framework's overall classification performance was improved by this method's ability to extract rich, discriminative features.

3.3.3 Histogram of Oriented Gradients (HOG)

The HOG approach was utilized in our work to extract features from dental images. The distribution of edge directions or intensity gradients in certain areas of an image is captured by the popular feature descriptor HOG. This technique is useful in dental analysis for detecting particular dental traits and diseases since it is very good at recognizing and describing shapes and structures within images [16] [31].

There are numerous essential processes that make up the HOG feature extraction process:

- ***Gradient Computation:***Calculating the image's gradient is the first step. With discrete approximations of the derivatives, the gradients may be computed. The Sobel operator, which calculates gradients in the x and y dimensions, is one of the most often used techniques [16].

$$G_x = I(x+1, y) - I(x-1, y)(Gradient\ in\ x - direction) \quad (15)$$

$$G_y = I(x, y+1) - I(x, y-1)(Gradient\ in\ y - direction) \quad (16)$$

It is possible to compute the direction θ and overall gradient magnitude G at each pixel as follows [16]:

$$G = \sqrt{G_x^2 + G_y^2} \quad (17)$$

$$\theta = \text{atan}\,2(G_y, G_x) \quad (18)$$

- ***Cell Division:*** The image is separated into cells, which are tiny, interconnected areas that are usually 8×8pixels. A gradient orientation histogram is calculated for every cell.
- ***Histogram of Orientations:*** The gradient orientation of each pixel in the cell determines how it contributes to the histogram. Typically, the histogram is separated into a predetermined number of bins, such as nine bins that represent orientations between 0° and 180° or 0° and 360°. The following formula may be used to determine each pixel's contribution to the histogram bin [31]:

$$Bin(k) = \sum_{p \in cell} (G_p . w_k) \quad (19)$$

Where w_k is a weight based on the gradient magnitude and G_p is the gradient magnitude at pixel p falling into the bin k.

- ***Block Normalization:***HOG utilizes normalization over bigger blocks of cells (usually 2×2 cells) to account for variations in lighting and contrast. To guarantee uniform feature scaling, the HOG feature vector is then normalized.The normalized vector V for a block with N cells can be calculated as follows [31]:

$$V = \frac{H}{\sqrt{\|H\|^2 + \epsilon^2}} \quad (20)$$

Where H is the concatenated histogram of the cells in the block, $\|H\|$ is the Euclidean norm of the histogram, and ϵ is a small constant added for numerical stability (typically $\epsilon = 1$).

- ***Feature Vector Construction:***The final HOG feature descriptor for the entire image is produced by concatenating the feature vectors from each block after the histograms of each block have been normalized.

A variety of dental problems were successfully classified using the HOG features that were taken from dental images. This method improved our diagnostic abilities by enabling us to recognize and differentiate between various tooth forms, edges, and structures.

Our methodology's use of HOG offered a reliable way to record and depict the structural and textural details seen in dental images. Our dental image segmentation and analysis framework performed better overall thanks to HOG's study of the gradient distribution in the images, which allowed for efficient categorization and detection of dental features.

3.3.4 Combined Feature Vector

The next important stage in our process is to construct a composite feature vector after feature extraction utilizing three different techniques: X-Feat, Gabor Filter-based Features, and HOG. The benefits of each distinct feature extraction technique are combined in this integrated feature vector to produce a thorough representation of the dental images that improves the precision and resilience of ensuing classification tasks.

The main driving force behind merging features from various extraction methods is their complimentary advantages:

- Cusps, ridges, and corners are examples of geometric structures and important locations that are captured by extreme features and offer vital information about the morphology and shape of teeth. These features are essential for distinguishing between tooth kinds and spotting structural abnormalities.
- Based on Gabor Filters In order to capture the spatial frequency and orientation properties that differentiate between good and poor dental diseases, features concentrate on texture information. They work especially well at capturing local texture patterns, which are crucial for identifying problems like enamel erosion or cavities.
- In order to identify the general form and borders of dental structures, HOG places a strong emphasis on the distribution of gradient orientations. By successfully highlighting the teeth's edges and contours, HOG improves the capacity to identify changes in dental morphology.

The various feature vectors from the X-Feat, Gabor Filter, and HOG methods are concatenated to create the composite feature vector. Let's use the following notation to represent the feature vectors from each technique:

- X_{feat}: The feature vector obtained from the Extreme Features extraction.
- G_{feat}: The feature vector obtained from the Gabor Filter extraction.
- H_{feat}: The feature vector obtained from the HOG extraction.

The combined feature vector $C_{feat}$is defined as:

$$C_{feat} = X_{feat} \oplus G_{feat} \oplus H_{feat}$$

(21)

Where the concatenation operation is shown by $\oplus$. This combines data from the three approaches to produce a high-dimensional feature vector.

Our classification model, which is based on a Bayesian-Optimized Random Forest method, uses the combined feature vector C_{feat} as its input. To increase classification accuracy and resilience, this model makes use of the rich and varied information included in the combined feature vector. The model may learn more complex patterns linked to different dental problems thanks to the synergy between the various feature kinds.

Our research improves the system's capacity to recognize and categorize dental features by using a comprehensive strategy that combines many feature extraction approaches. By addressing the intricacies present in dental imaging, this integrated technique improves diagnostic performance and reliability.

A key component of our technique is the creation of the combined feature vector, which combines the complementing advantages of HOG, Gabor Filter-based Features, and X-Feat. This thorough depiction improves dental image analysis's classification ability, making it an effective tool for identifying and diagnosing dental disorders. The efficiency of our strategy in developing the area of dental diagnostics is demonstrated by the successful integration of various feature extraction techniques.

3.4 *Bayesian-Optimized Random Forest Classifier for Caries Detection and Classification*

In this study, the primary machine learning model for identifying and categorizing caries (tooth decay) in dental images is a Bayesian-Optimized Random Forest Classifier [32]. A strong ensemble-based classifier with a reputation for high accuracy and resistance to overfitting is the Random Forest (RF) method. Because of its capacity to manage intricate, non-linear connections within the data, RF is especially useful in the context of caries detection, where images display notable heterogeneity in texture, shape, and illumination. We further improve the performance of the RF model by fine-tuning hyperparameters through the integration of Bayesian optimization, which guarantees optimal classification accuracy over a range of caries stages and situations.

3.4.1 Random Forest Classifier

A random subset of the data and features is used to train each decision tree in the Random Forest classifier, which is an ensemble of trees [33]. It is employed in our study to categorize dental images into various caries stages or other problems. The output from several decision trees is combined to establish the classifier's prediction, which lowers variance and increases accuracy. Because Random Forest can handle huge feature spaces produced from dental images without losing interpretability or overfitting the model, it is a good choice for the caries classification task.

A Random Forest classifier functions mathematically as follows:

- ***Decision Tree Construction:*** A random subset of the training data D_{subset}, which is produced via bootstrap sampling from the entire dataset D, is used to train each Random Forest decision tree. With $m = 1,2,\ldots,M$ and M being the total number of trees, for every tree T_m [33]:

$$T_m = train(D_{subset}), \;\; D_{subset} \subseteq D$$

(22)

Based on the feature set that was taken from dental images (such as Gabor filters, Extreme Features, and HOG features), each tree T_m learns to identify an image in this case.

- ***Voting Mechanism:*** The Random Forest averages the predictions made by each tree in the forest once all the trees have been taught. The most common class predicted by each tree for a given test image x_{test} is the anticipated class $\hat{y}_{test}$ [33]:

$$\hat{y}_{test} = \text{mode}\big(T_1(x_{test}), T_2(x_{test}), \ldots, T_M(x_{test})\big)$$

(23)

Based on the decision trees' majority vote, the test image is classified as either healthy, in the early stages of caries, moderate caries, or advanced caries in the case of caries detection.

3.4.2 Bayesian Optimization for Hyperparameter Tuning

Choosing the ideal collection of hyperparameters, such as the number of trees M, the maximum depth of each tree d_{max}, and the amount of features f_{split} taken into account for each split, is one of the main difficulties with the Random Forest method. Overfitting or less-than-ideal performance might result from poorly selected hyperparameters. In order to solve this, we use Bayesian optimization to determine the best set of

hyperparameters for our particular caries classification problem.

Finding the ideal hyperparameter configuration is the aim of Bayesian optimization, which aims to optimize classification accuracy. This is accomplished by employing a probabilistic model, usually a Gaussian process (GP), to represent the link between the hyperparameters and the classifier's performance. Through iterative exploration of the hyperparameter space and the selection of attractive configurations based on the GP model, Bayesian optimization works.

Formally, let $\mathcal{L}(\mathcal{H})$ stand for the objective function (such as classification accuracy) to be maximized, and let $\mathcal{H} = \{M, d_{max}, f_{split}, \dots\}$ represent the collection of hyperparameters to optimize. The goal of Bayesian optimization is to [32]:

$$\mathcal{H}^* = \arg\max_{\mathcal{H}} \mathcal{L}(\mathcal{H})$$

(24)

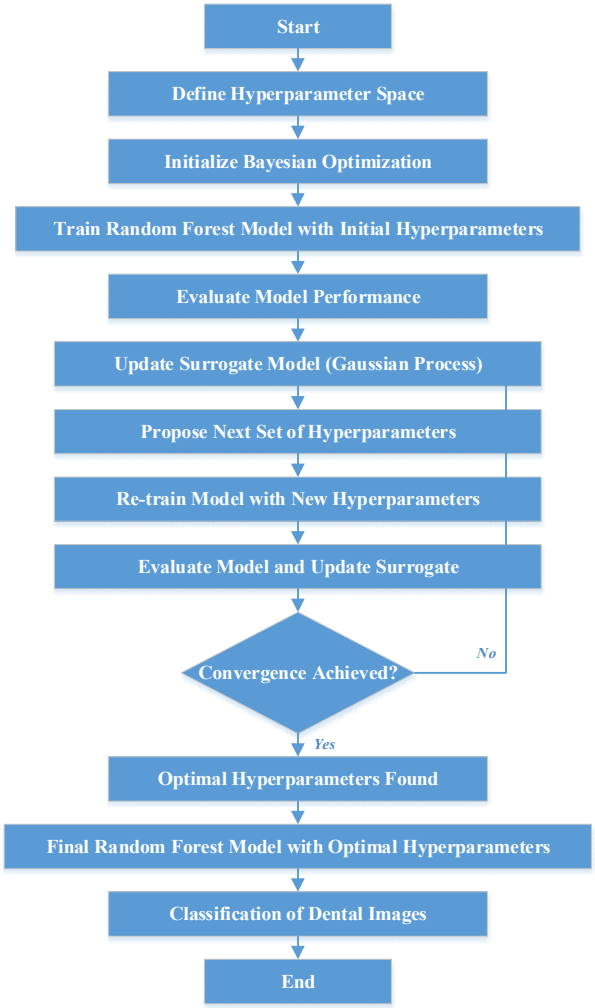

Figure 2: Bayesian Optimization Approach for Random Forest Classifier

The following is a summary of the Bayesian optimization process:

1. ***Surrogate Model Construction:***To represent the objective function $\mathcal{L}(\mathcal{H})$, a Gaussian process $GP(\mathcal{H}, \mathcal{L})$ is built, incorporating uncertainty in unexplored areas of the hyperparameter space.

2. ***Acquisition Function:*** The next hyperparameter configuration to be evaluated is determined by an acquisition function $a(\mathcal{H})$, such as Upper Confidence Bound (UCB) or Expected Improvement (EI). This strikes a compromise between exploitation (concentrating on promising regions) and exploration (testing various hyperparameter setups).
3. ***Evaluation and Update:*** The selected hyperparameter set is used to train and assess the classifier, and the GP model is modified in light of the performance that is seen. Until convergence or a certain computing budget is reached, this process is repeated.

Bayesian optimization is used in our study to adjust important hyperparameters like:

- The ensemble's size is controlled by the number of trees (M).
- Maximum tree depth (d_{max}): Controls each tree's level of complexity.
- The number of features that are taken into account while splitting at each node is determined by the number of features (f_{split}).

We guarantee optimal performance of the Random Forest classifier, especially for caries detection and classification, by adjusting these parameters.

The flow diagram in Figure 2 shows how to use Bayesian optimization to optimize a Random Forest classifier's hyperparameters step-by-step. First, the optimization is initialized and the hyperparameter space is defined. Until convergence is attained, iteratively training the Random Forest model with suggested hyperparameters, assessing its performance, and updating the surrogate model. The final model is trained and used for dental image classification when the ideal hyperparameters have been determined.

This research is a useful tool for enhancing dental diagnostics as it uses the Bayesian-Optimized Random Forest to identify and categorize caries with exceptional accuracy and efficiency.

IV. RESULTS AND DISCUSSION

4.1 Dental Condition Dataset

A vast collection of dental images selected to aid in study and analysis on a range of oral health issues is known as the Dental Condition Dataset. Our study is mainly concerned with the detection and classification of caries (tooth decay) [34]. For the purpose of recognizing and classifying dental caries as well as other pertinent dental disorders, this dataset offers a crucial basis for training and validating machine learning models [34].

Dataset Overview:

- **Image Categories:** Although there are many other dental problems in the dataset, our study mostly uses the images of cavities. The following categories are used to arrange the dataset:
- **Caries:** These images, which are a major focus of our study, show different phases of dental decay, such as cavities and carious lesions, which are essential for creating our models for detection and categorization.
- **Calculus:** Images of tartar accumulation that provide as additional information to differentiate between various dental disorders.
- **Gingivitis:** Images showing inflammation of the gums can help with a more comprehensive examination of dental health.
- **Tooth Discoloration:** Images of stained teeth are presented to show variances in texture and color.
- **Ulcers:** Images of mouth ulcers that help identify anomalies in soft tissues.
- **Hypodontia:** These images show missing teeth and provide more structural information for classifying dental conditions.

Image Sources:Image Sources: To ensure a wide range of dental problems and patient demographics, the dataset is obtained from a number of hospitals and reputable dentistry websites. This guarantees that our caries detection models employ a variety of data that is representative of actual situations.

Annotation and Augmentation:Every image has been painstakingly annotated, with bounding boxes indicating certain regions of interest, such carious lesions. Furthermore, data augmentation methods including rotation, flipping, scaling, and noise addition have been used to increase the model's resilience and capacity for generalization, particularly in tasks involving the identification of dental cavities.

The dataset's example images are displayed in Figure 3.

Figure 3: Illustration of Sample Images from Dental Condition Dataset [34]

4.2 Evaluation Parameters

Table 1: Evaluation Parameters

TP (True Positive)	Represents the count of dental images correctly classified as showing the presence of caries (tooth decay).
TN (True Negative)	Indicates the number of dental images correctly classified as not having caries (healthy teeth).
FP (False Positive)	Represents the number of dental images incorrectly classified as showing caries when they were actually healthy.
FN (False Negative)	Indicates the number of dental images incorrectly classified as healthy when they actually showed the presence of caries.

$$Accuracy = \frac{TP + TN}{TP + TN + FP + FN} \quad (25)$$

$$Precision = \frac{TP}{TP + FP} \quad (26)$$

$$Sensitivity = \frac{TP}{TP + FN}$$

(27)

$$Specificity = \frac{TN}{TN + FN}$$

(28)

$$ErrorRate = \frac{FP + FN}{TP + TN + FP + FN}$$

(29)

$$FalsePositiveRate(FPR) = \frac{FP}{FP + TN}$$

(30)

$$F - Score = \frac{2TP}{2TP + FP + FN}$$

(31)

4.3 Results

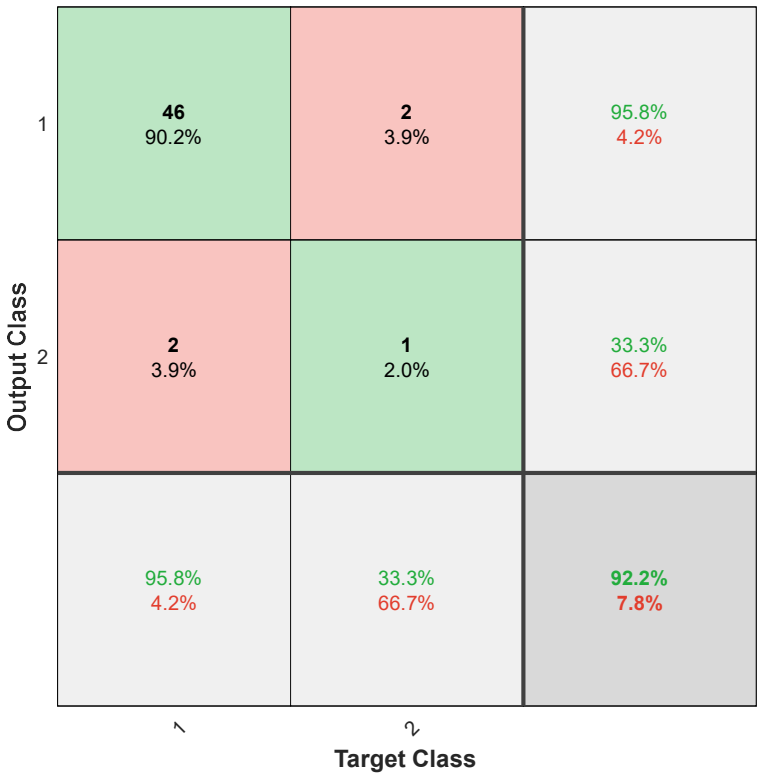

Figure 4: Confusion matrix plot for proposed caries detection using Gabor filter based approach

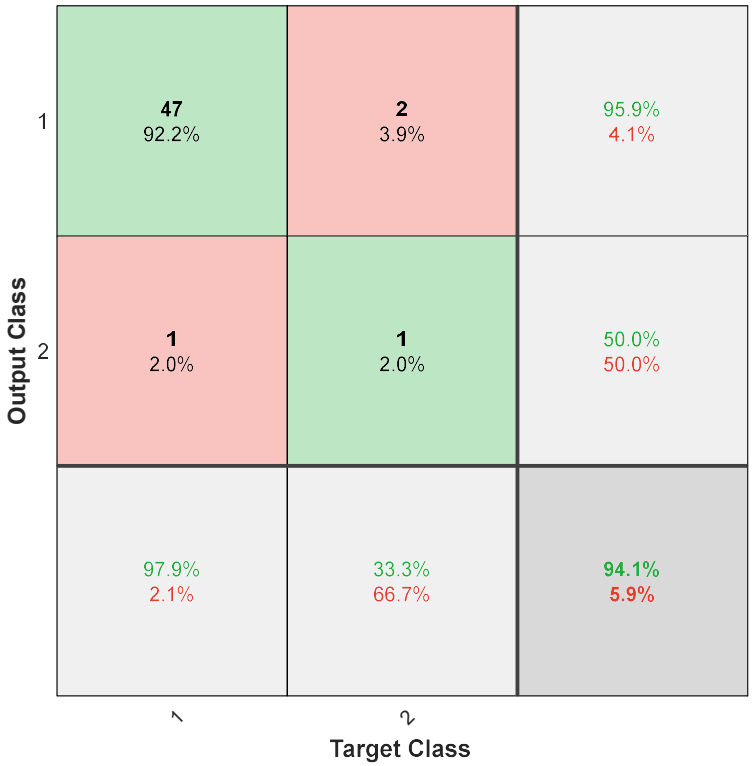

Figure 5: Confusion matrix plot for proposed caries detection using Extreme features based approach

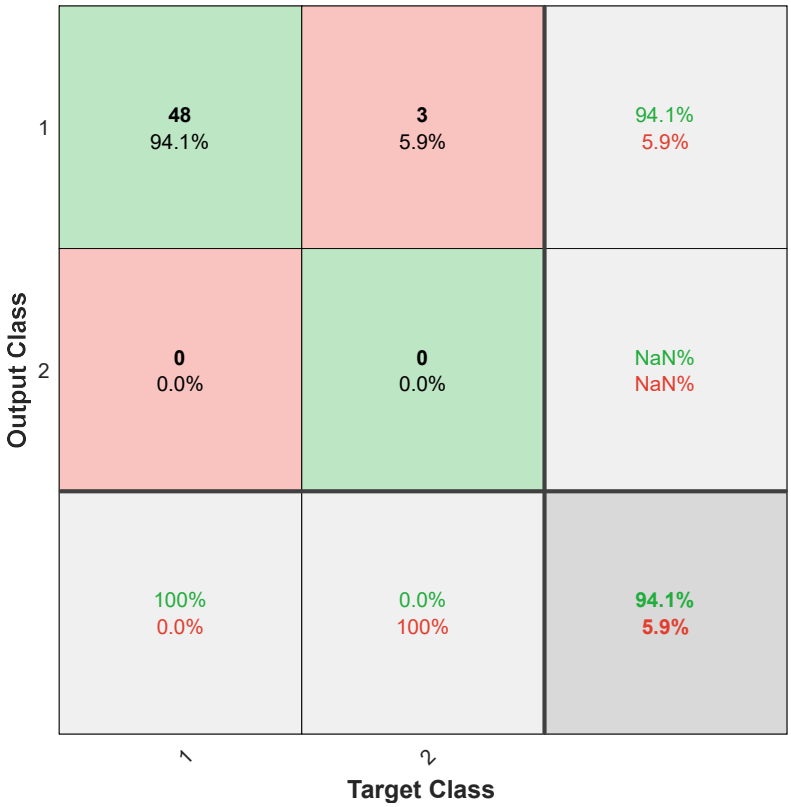

Figure 6: Confusion matrix plot for proposed caries detection using HOG features based approach

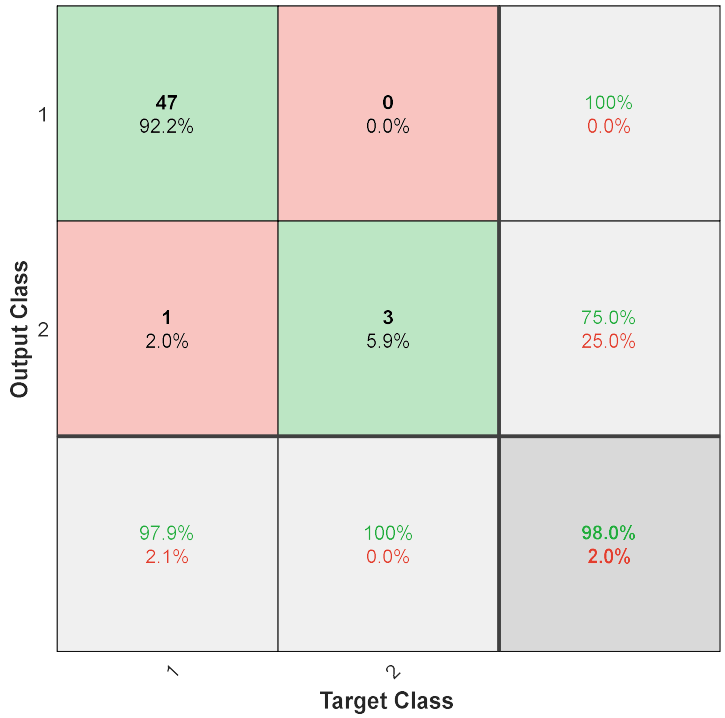

Figure 7: Confusion Matrix Plot for Proposed Caries Detection using Hybrid Features based Random Forest Approach

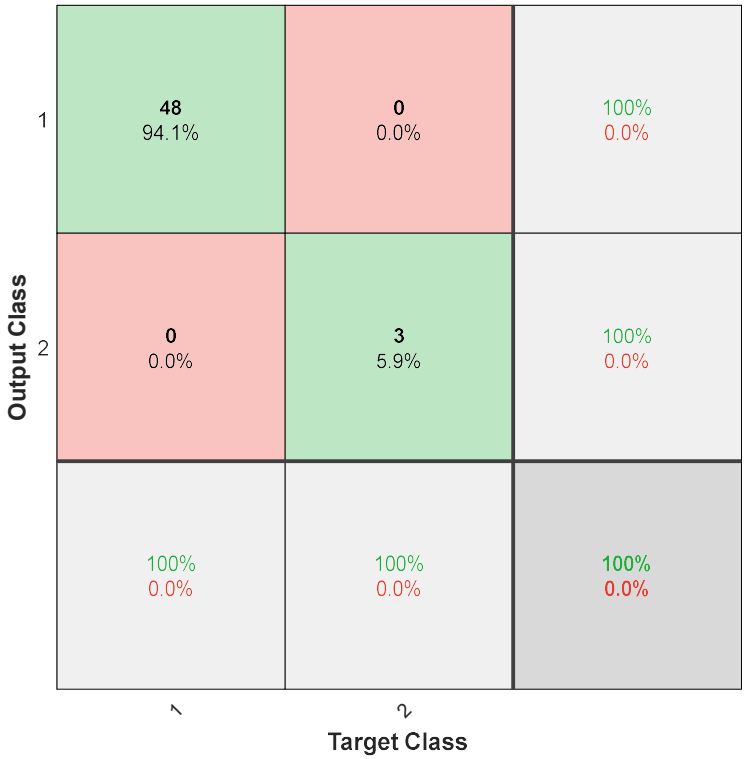

Figure 8: Confusion Matrix Plot for Proposed Caries Detection using Hybrid Features based Bayesian-Optimized Random Forest Approach

Table 2: Comparative analysis of proposed caries detection results with various features extraction methods

Parameter	Gabor Filter	Extreme Features	HOG Features	Hybrid features + RF	Hybrid features + Bayesian-Optimized RF
Accuracy	92.16%	94.12%	94.12%	98.04%	98.08%
Error	7.84%	5.88%	5.88%	1.96%	1.92%
Sensitivity	92.16%	94.12%	94.12%	98.04%	98.08%
Specificity	92.16%	94.12%	94.12%	98.04%	98.08%
Precision	92.16%	94.12%	94.12%	98.04%	98.08%
False Positive Rate	7.84%	5.88%	5.88%	1.96%	1.92%
F1 Score	92.16%	94.12%	94.12%	98.04%	98.08%
Matthews Correlation Coefficient (MCC)	84.31%	88.24%	88.24%	96.08%	96.15%
Kappa	84.31%	88.24%	88.24%	96.08%	96.15%

A comparison of caries detection performance utilizing different feature extraction techniques is shown in Table 2. Across a range of parameters, the suggested techniques that combine hybrid features with Random Forest (RF) and Bayesian-Optimized RF classifiers continuously beat more straightforward feature extraction techniques like Gabor Filter, Extreme Features, and HOG Features. The hybrid methods have the lowest mistake and false positive rates (about 1.9%), while achieving the best accuracy, sensitivity, specificity, and precision (about 98%). The Hybrid + Bayesian-Optimized RF performed best overall, with 98.08% accuracy, 96.15% MCC, and 96.15% Kappa, demonstrating high reliability and robustness in caries detection when compared to other methods.

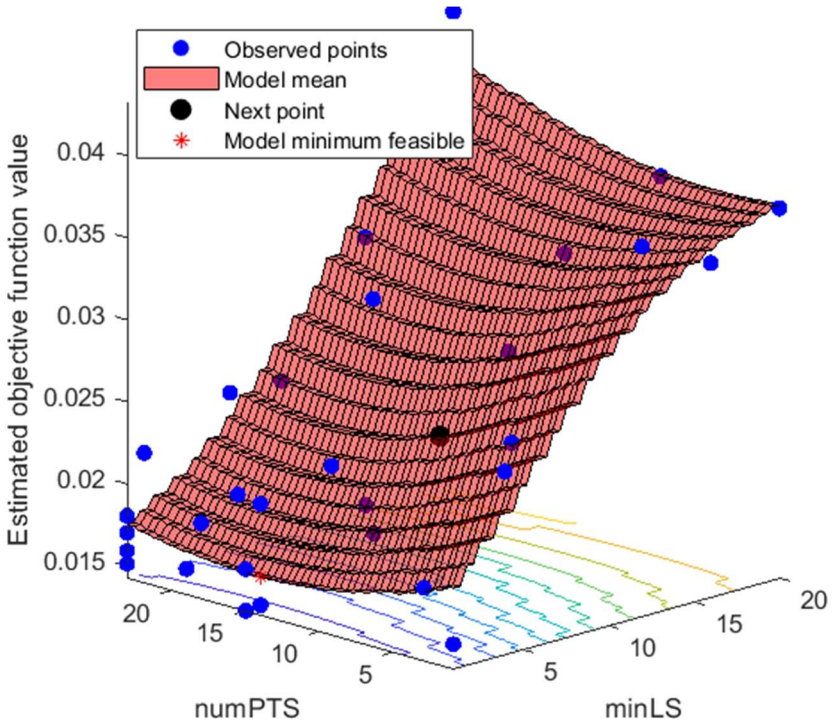

Figure 9: Objective function model

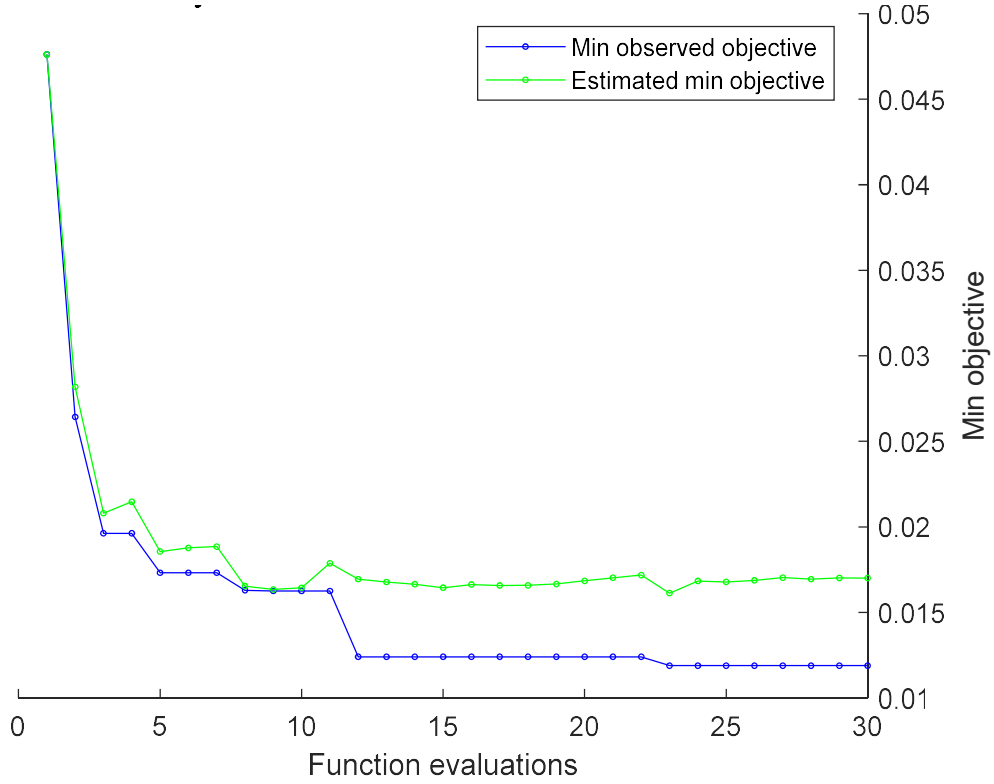

Figure 10: Minimum objective vs. number of function evaluations

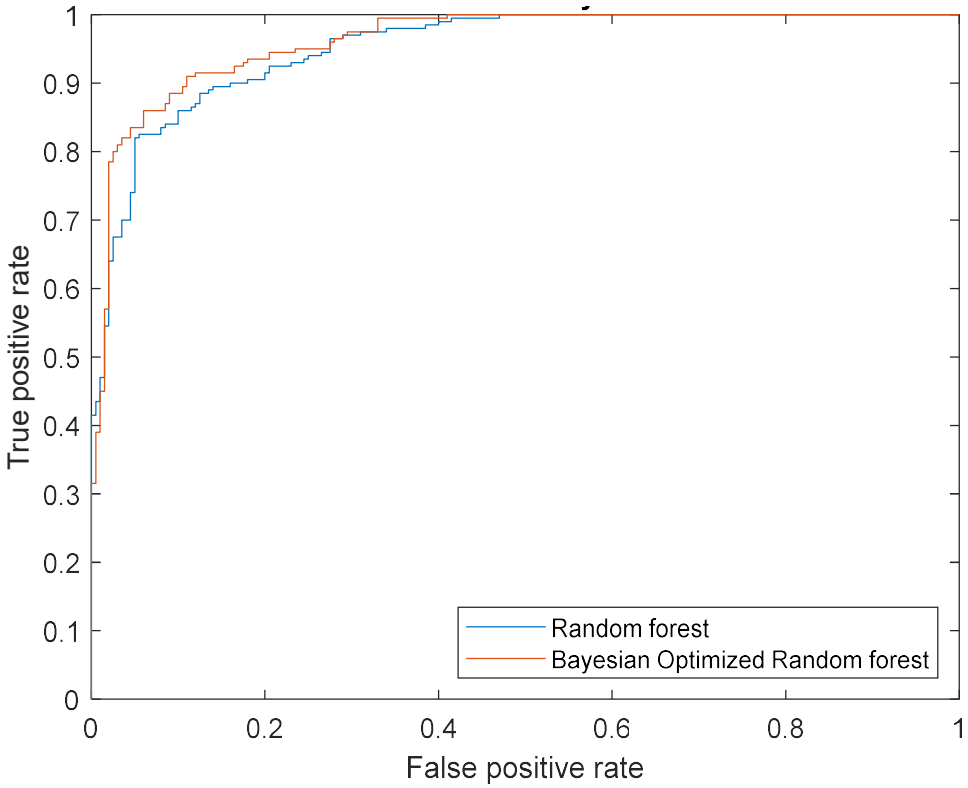

Figure 11: ROC curve for Random Forest and Bayesian-optimized Random forest

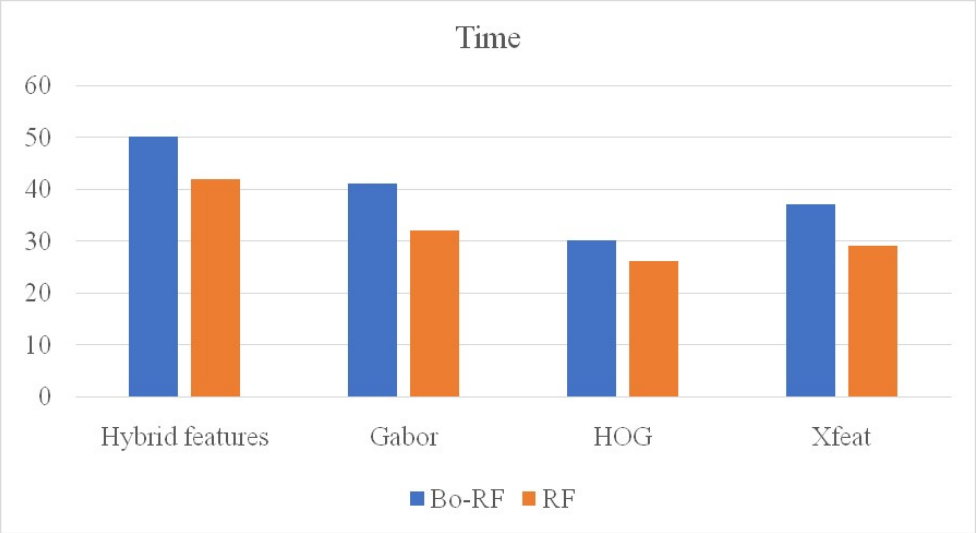

Figure 12: Training time in seconds with different features and classifiers

The observable variations in training duration across different settings are clearly depicted in Figure 12. The training time comparison between the hybrid features and normalized hybrid features is shown in these figures. Both corpus and polarity were included as features in the assessment. One noteworthy accomplishment is the significant decrease in training time that our approach provides. In every situation, our model continuously demonstrated a training time that was roughly less than that of the hybrid model, and in several cases, it substantially doubled in speed. Crucially, accuracy was maintained despite the increased speed. Conversely, this suggested model was able to achieve greater levels of accuracy.

Table 3: Comparative analysis of the proposed approach with previous research works

Methods	Accuracy	Sensitivity	Precision	F-Score
[26] U-Net for Infection Detection	94.3%	–	–	–
[27] CBCT for Molar Root Classification	86.9%	–	–	–
[28] CNN for Tooth Detection	92.08%	–	–	–
Proposed work (Hybrid features + RF)	**98.04%**	**98.04%**	**98.04%**	**98.04%**
Proposed work (Hybrid features + Bayesian-Optimized RF)	**98.08%**	**98.08%**	**98.08%**	**98.08%**

The proposed hybrid feature-based caries detection method with Random Forest (RF) and Bayesian-Optimized RF classifiers is contrasted with earlier dental imaging research techniques in Table 3. With the maximum accuracy, sensitivity, precision, and F-Score of around 98.08% and 98.04%, respectively, the proposed methods perform noticeably better than previous techniques. On the other hand, previous techniques such as CNN for tooth detection, CBCT for molar root classification, and U-Net for infection detection claim accuracy values of 94.3%, 86.9%, and 92.08%, respectively, without disclosing sensitivity, precision, or F-Score. Significant progress in automated caries detection is shown by this performance increase, which highlights the proposed approach's strong accuracy and consistency across all important measures.

V. CONCLUSION

A significant improvement in dental image analysis, namely for automated caries identification, is demonstrated by the methods presented in this research. The model consistently outperforms both newer machine learning-based techniques and conventional diagnostic techniques in terms of accuracy, sensitivity, specificity, and precision by utilizing a hybrid feature extraction approach in conjunction with Random Forest (RF) and Bayesian-Optimized RF classifiers. The use of hybrid features improves the model's capacity to differentiate across dental diseases by efficiently retrieving a variety of geometric and textural features. This is further enhanced by Bayesian hyperparameter adjustments, which enables the classifier to function with exceptional

stability and adaptability in a variety of settings, leading to a peak accuracy of 98.08%, which surpasses previous research benchmarks. Furthermore, as demonstrated by the comparison study, the method significantly reduces training time without reducing accuracy, making it a workable and effective alternative for clinical situations. These developments give dentists a dependable tool for prompt, precise diagnosis, which is essential for efficient treatment planning and improved patient outcomes in the field of dentistry. Setting a new benchmark for precision as well as efficiency in caries diagnosis, the study not only advances the area of dental image analysis but also creates opportunities for future advancements in automated dental diagnostics. The model's generalization and diagnosis accuracy can be further improved in subsequent work by using more varied datasets, such as intraoral scans and 3D dental images.

REFERENCES

[1] Elżbieta Machoy, M., Szyszka-Sommerfeld, L., Vegh, A., Gedrange, T. and Woźniak, K., 2020. The ways of using machine learning in dentistry. *Advances in Clinical & Experimental Medicine*, *29*(3).

[2] Rimi, I.F., Arif, M.A.I., Akter, S., Rahman, M.R., Islam, A.S. and Habib, M.T., 2022. Machine learning techniques for dental disease prediction. *Iran Journal of Computer Science*, *5*(3), pp.187-195.

[3] Muresan, M.P., Barbura, A.R. and Nedevschi, S., 2022, September. Teeth detection and dental problem classification in panoramic X-ray images using deep learning and image processing techniques. In *2022 IEEE 16th International Conference on Intelligent Computer Communication and Processing (ICCP)* (pp. 457-463). IEEE.

[4] Ward, I.R., Laga, H. and Bennamoun, M., 2022. RGB-D image-based object detection: from traditional methods to deep learning techniques. *RGB-D Image Analysis and Processing*, pp.169-201.

[5] Patil, S., Albogami, S., Hosmani, J., Mujoo, S., Kamil, M.A., Mansour, M.A., Abdul, H.N., Bhandi, S. and Ahmed, S.S., 2022. Artificial intelligence in the diagnosis of oral diseases: applications and pitfalls. *Diagnostics*, *12*(5), p.1029.

[6] Nambiar, R. and Nanjundegowda, R., 2024. A Comprehensive Review of AI and Deep Learning Applications in Dentistry: From Image Segmentation to Treatment Planning. *Journal of Robotics and Control (JRC)*, *5*(6), pp.1744-1752.

[7] Imak, A., Celebi, A., Siddique, K., Turkoglu, M., Sengur, A. and Salam, I., 2022. Dental caries detection using score-based multi-input deep convolutional neural network. *IEEE Access*, *10*, pp.18320-18329.

[8] Rubiu, G., Bologna, M., Cellina, M., Cè, M., Sala, D., Pagani, R., Mattavelli, E., Fazzini, D., Ibba, S., Papa, S. and Alì, M., 2023. Teeth segmentation in panoramic dental X-ray using mask regional convolutional neural network. *Applied Sciences*, *13*(13), p.7947.

[9] Zhang, X., 2024, July. Integrating U-net and Multi-Model Approaches for Accurate Dental Occlusal Surface and Caries Detection. In *2024 3rd International Conference on Robotics, Artificial Intelligence and Intelligent Control (RAIIC)* (pp. 33-40). IEEE.

[10] Yang, S., Kim, K.D., Ariji, E. and Kise, Y., 2024. Generative adversarial networks in dental imaging: a systematic review. *Oral Radiology*, *40*(2), pp.93-108.

[11] Li, P., Gao, C., Liu, F., Meng, D. and Yan, Y., 2023. THISNet: Tooth Instance Segmentation on 3D Dental Models via Highlighting Tooth Regions. *IEEE Transactions on Circuits and Systems for Video Technology*.

[12] Harsh, P., Chakraborty, R., Tripathi, S. and Sharma, K., 2021, June. Attention U-Net architecture for dental image segmentation. In *2021 International Conference on Intelligent Technologies (CONIT)* (pp. 1-5). IEEE.

[13] Rajee, M.V. and Mythili, C., 2023. Dental image segmentation and classification using inception Resnetv2. *IETE Journal of Research*, *69*(8), pp.4972-4988.

[14] Zheng, Q., Gao, Y., Zhou, M., Li, H., Lin, J., Zhang, W. and Chen, X., 2024. Semi or fully automatic tooth segmentation in CBCT images: a review. *PeerJ Computer Science*, *10*, p.e1994.

[15] Zanini, L.G.K., Rubira-Bullen, I.R.F. and dos Santos Nunes, F.D.L., 2024. Enhancing dental caries classification in CBCT images by using image processing and self-supervised learning. *Computers in Biology and Medicine*, *183*, p.109221.

[16] Janardanan, R.P. and Logeswaran, R., 2019. Dental Radiograph Segmentation and Classification—A Comparative Study of Hu's Moments and Histogram of Oriented Gradients. *Journal of Computational and Theoretical Nanoscience*, *16*(8), pp.3612-3616.

[17] Vicory, J., Chandradevan, R., Hernandez-Cerdan, P., Huang, W.A., Fox, D., Qdais, L.A., McCormick, M., Mol, A., Walter, R., Marron, J.S. and Geha, H., 2021, February. Dental microfracture detection using wavelet features and machine learning. In *Medical Imaging 2021: Image Processing* (Vol. 11596, pp. 484-492). SPIE.

[18] Sukegawa, S., Fujimura, A., Taguchi, A., Yamamoto, N., Kitamura, A., Goto, R., Nakano, K., Takabatake, K., Kawai, H., Nagatsuka, H. and Furuki, Y., 2022. Identification of osteoporosis using ensemble deep learning model with panoramic radiographs and clinical covariates. *Scientific reports*, *12*(1), p.6088.

[19] Elgarba, B.M., Van Aelst, S., Swaity, A., Morgan, N., Shujaat, S. and Jacobs, R., 2023. Deep learning-based segmentation of dental implants on cone-beam computed tomography images: A validation study. *Journal of Dentistry*, *137*, p.104639.

[20] Jang, T.J., Kim, K.C., Cho, H.C. and Seo, J.K., 2021. A fully automated method for 3D individual tooth identification and segmentation in dental CBCT. *IEEE transactions on pattern analysis and machine intelligence*, *44*(10), pp.6562-6568.

[21] Vigil, M.A., Gowri, V., Ramesh, S.S., Praba, M.B. and Sabitha, P., 2024. ADGRU: Adaptive DenseNet with gated recurrent unit for automatic diagnosis of periodontal bone loss and stage periodontitis with tooth segmentation mechanism. *Clinical Oral Investigations*, *28*(11), p.614.

[22] Gondara, L., 2022, December. Medical image denoising using convolutional denoising autoencoders. In *2022 IEEE 16th international conference on data mining workshops (ICDMW)* (pp. 241-246). IEEE.

[23] Zhicheng, H., Yipeng, W. and Xiao, L., 2024. Deep Learning-Based Detection of Impacted Teeth on Panoramic Radiographs. *Biomedical Engineering and Computational Biology*, *15*, p.11795972241288319.

[24] Van der Velden, B.H., Kuijf, H.J., Gilhuijs, K.G. and Viergever, M.A., 2022. Explainable artificial intelligence (XAI) in deep learning-based medical image analysis. *Medical Image Analysis*, *79*, p.102470.

[25] Kustra, J., de Jager, M., Jalba, A. and Telea, A., 2020, January. A medial point cloud based algorithm for dental cast segmentation. In *2020 IEEE International Conference on Consumer Electronics (ICCE)* (pp. 331-334). IEEE.

[26] Lee, J.H., Kim, D.H., Jeong, S.N. and Choi, S.H., 2022. Detection and diagnosis of dental caries using a deep learning-based convolutional neural network algorithm. *Journal of dentistry*, *77*, pp.106-111.

[27] Hiraiwa, T., Ariji, Y., Fukuda, M., Kise, Y., Nakata, K., Katsumata, A., Fujita, H. and Ariji, E., 2022. A deep-learning artificial intelligence system for assessment of root morphology of the mandibular first molar on panoramic radiography. *Dentomaxillofacial Radiology*, *48*(3), p.20180218.

[28] Silva, G., Oliveira, L. and Pithon, M., 2021. Automatic segmenting teeth in X-ray images: Trends, a novel data set, benchmarking and future perspectives. *Expert Systems with Applications*, *107*, pp.15-31.

[29] Potje, G., Cadar, F., Araujo, A., Martins, R. and Nascimento, E.R., 2024. XFeat: Accelerated Features for Lightweight Image Matching. In *Proceedings of the IEEE/CVF Conference on Computer Vision and Pattern Recognition* (pp. 2682-2691).

[30] Jusman, Y., Nur'aini, M.A. and Puspitasari, S., 2022, December. Gabor Filter-Based Caries Image Feature Analysis Using Machine Learning. In *2022 5th International Seminar on Research of Information Technology and Intelligent Systems (ISRITI)* (pp. 514-519). IEEE.

[31] Albahbah, A.A., Esmeda, L.A. and Almajrabi, T., 2021. An Effective Method for Caries Detection In Panoramic Dental Images. *Journal of Basic Sciences*, *34*(1), pp.96-113.

[32] Rajesh, P.K., Shreyanth, S., Sarveshwaran, R. and Nithin Chary, V., 2023, April. Bayesian-Optimized Random Forest Classifier for Improved Credit Card Fraud Detection: Overcoming Challenges and Limitations. In *XVIII International Conference on Data Science and Intelligent Analysis of Information* (pp. 205-214). Cham: Springer Nature Switzerland.

[33] Singh, S.B., Laishram, A., Thongam, K. and Singh, K.M., 2024. A Random Forest-based Automatic Classification of Dental Types and Pathologies using Panoramic Radiography Images: Dental Types and Anomalies Classification Using Random Forest. *Journal of Scientific & Industrial Research (JSIR)*, *83*(5), pp.531-543.

[34] Dental Condition Dataset, Online available at: https://www.kaggle.com/datasets/salmansajid05/oral-diseases